One-dimensional quantum transport affected by a background medium: Fluctuations versus correlations

S. Ejima and H. Fehske
Institut für Physik, Ernst-Moritz-Arndt-Universität Greifswald, 17489 Greifswald, Germany
(Received 17 July 2009; revised manuscript received 31 August 2009; published 1 October 2009)

We analyze the spectral properties of a very general two-channel fermion-boson transport model in the insulating and metallic regimes and the signatures of the metal-insulator quantum phase transition in between. To this end we determine the single-particle spectral function related to angle-resolved photoemission spectroscopy, the momentum distribution function, the Drude weight, and the optical response by means of a dynamical (pseudosite) density-matrix renormalization group technique for the one-dimensional half-filled band case. We show how the interplay of correlations and fluctuations in the background medium controls the charge dynamics of the system, which is a fundamental problem in a great variety of advanced materials.

DOI: 10.1103/PhysRevB.80.155101 PACS number(s): 71.10.Fd, 71.30.+h, 71.10.Hf

I. INTRODUCTION

Charge transport normally takes place in some background medium. To understand how the environment affects the moving carrier and vice versa is a difficult question and in this generality at present perhaps one of the most heavily debated issues in condensed matter physics. Here the term "background" describes a variety of situations. We can think of the motion of a hole through an ordered insulator.[1] Examples are the high-T_c cuprates and the colossal magnetoresistive manganates, with a background of spins and orbitals, respectively, forming a pattern of alternating order. Then, as the hole moves, it disrupts the order of the background, which on its part hinders the particle transfer. Nevertheless coherent particle transport may occur but on a strongly renormalized energy scale. The new quasiparticles formed in the cuprates and manganates are spin or orbital polarons.[2–4] Another situation concerns a charge carrier coupled to a deformable background. Here, if the interaction with phonons is strong, the particle has to carry a phonon cloud through the medium. The outcome might be a "self-trapped" small lattice polaron.[5] In this case hopping transport, accompanied by phonon emission and absorption processes, evolves as the dominant transport channel.

So far we have considered a single particle only. It is quite obvious that the problem becomes even more involved if the particle density increases. Then the interrelation between charge carriers and background medium may drive quantum phase transitions. The appearance of ferromagnetism in the three-dimensional manganates, superconductivity in the quasi-two-dimensional (2D) cuprates, or charge-density-wave (CDW) states in one-dimensional (1D) halogen-bridged transition-metal complexes are prominent examples.[6] In the theoretical description of these strongly correlated systems an additional difficulty arises: the particles which are responsible for charge transport and the order phenomena of the background are the same. As a consequence, on a microscopic level, rather involved many-particle models result, which incorporate the coupling between charge, spin, orbital, and lattice degrees of freedom.[4,7] Naturally this prevents an exact solution of the problem even in reduced dimensions.

II. MODEL AND METHOD

A way out might be the construction of simplified transport models, which capture the basic mechanisms of quantum transport in a background medium in an effective way. Along this line a quantum transport model has been proposed recently[8,9]

$$H = -t_b \sum_{\langle i,j \rangle} f_j^\dagger f_i (b_i^\dagger + b_j) - \lambda \sum_i (b_i^\dagger + b_i) + \omega_0 \sum_i b_i^\dagger b_i, \quad (1)$$

which mimics the correlations inherent to a spinful fermionic many-particle system by a boson-affected hopping of spinless particles $\propto t_b$ (see Fig. 1). In the model (1), a fermion $f_i^{(\dagger)}$ creates (or absorbs) a local boson $b_i^{(\dagger)}$ every time it hops, which corresponds to a local excitation in the background with a certain energy ω_0. Because of quantum fluctuations the distortions are able to relax $\propto\lambda$. A unitary transformation $b_i \to b_i + \lambda/\omega_0$ replaces this term by second transport channel $H_f = -t_f \Sigma_{\langle i,j \rangle} f_j^\dagger f_i$, describing unaffected fermionic transfer, however with a renormalized amplitude $t_f = 2\lambda t_b/\omega_0$. It has been shown[9] that coherent propagation of a fermion is possible even in the limit $\lambda = t_f = 0$ by means of a six-step vacuum-restoring hopping process

$$R_i^{(6)} = L_{i+2}^\dagger L_{i+1}^\dagger R_i^\dagger L_{i+2} R_{i+1} R_i, \quad (2)$$

where $R_i^\dagger = f_i^\dagger f_{i+1} b_i$ and $L_i^\dagger = f_i^\dagger f_{i-1} b_i$. Note that $R_i^{(6)}$ acts as direct next-nearest-neighbor (NNN) transfer "$f_{i+2}^\dagger f_i$," in complete analogy to the "Trugman path" of a hole in a 2D Néel-ordered spin background.[10]

The model (1) has been solved in the single-particle sector ($N_e = 1$) by exact diagonalization,[9] using a basis construction for the fermion-boson (many-particle) Hilbert space that is variational for an infinite lattice ($N = \infty$).[11] The transport behavior was found to be surprisingly complex, reflecting the properties of both spin and lattice polarons in t-J- and Holstein-type models.

For the 1D half-filled band sector ($N_e = N/2$), evidence for a metal insulator transition comes from small cluster diagonalizations.[12] Quite recently the ground-state phase diagram of the model (1) has been mapped out in the whole $\lambda - \omega_0$ plane,[13] using a density-matrix renormalization group (DMRG) technique.[14] A quantum phase transition between a

 ©2009 The American Physical Society

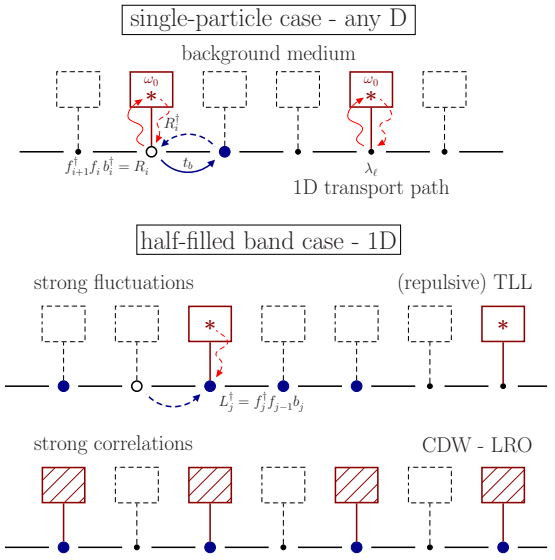

FIG. 1. (Color online) Schematic of quantum transport in a background medium. The background could represent a magnetically, orbitally, or charge ordered lattice but also a heat bath or certain chemical side groups. Then the proposed transport model (1) describes a very general situation: as a charge carrier (●) moves along a 1D transport path it creates an excitation with energy ω_0 (*) in the background medium at the site it leaves or annihilates an existing excitation at the site it enters. It is a plausible assumption that the (de)excitation of the background can be parameterized as a bosonic degree of freedom. In the case of spin deviations, orbital fluctuations, or lattice vibrations, the bosons might be viewed as a Schwinger-bosons, orbitons or phonons. Of course, any distortion of the background can heal out by quantum fluctuations. Accordingly the λ term allows for spontaneous boson creation and annihilation processes. The upper panel displays the single-particle case. Depending on the model parameters quasifree, diffusive, or boson-assisted transport takes place (Ref. 9). The latter case corresponds, e.g., to the motion of a hole through an ordered antiferromagnetic insulator. The lower panel shows the half-filled band case. Here, for spinless fermions in 1D, a repulsive Tomonaga-Luttinger liquid evolves, provided the excitations of the background are energetically inexpensive ($\omega_0 < \omega_{0,c}$) or will readily relax [$\lambda > \lambda_c(\omega_0)$]. This defines the fluctuation dominated regime. By contrast, strong background correlations, which develop for large ω_0 and small $\lambda \ll t_b$ tend to immobilize the charge carriers and even may drive a metal-insulator transition by establishing CDW long-range order (Refs. 12 and 13).

Tomonaga-Luttinger liquid (TLL) and CDW was proven to exist. A complementary study of the dynamical properties of the system is therefore desirable.

In the present work, we employ the dynamical DMRG (DDMRG) method[15] in order to investigate the effects of background fluctuations and correlations on the dynamics of charge carriers in the framework of the 1D half-filled fermion-boson model (1). Thereby the focus is on the wave-vector resolves single-particle spectral function probed by angle-resolved photoemission spectroscopy (ARPES) and on the optical conductivity probed, e.g., by reflectivity measurements.

In general the dynamic response of a quantum system described by a time-independent Hamiltonian H is given by the imaginary part of correlation functions of type

$$A_O(\omega) = \lim_{\eta \to 0} \frac{1}{\pi} \langle \psi_0 | O^\dagger \frac{\eta}{(E_0 + \omega - H)^2 + \eta^2} O | \psi_0 \rangle, \qquad (3)$$

where the operator O identifies the physical quantity of interest. $|\psi_0\rangle$ and E_0 give the ground-state wave function and energy of H. The small $\eta > 0$ shifts the poles of the related Green's function $G_O(\omega + i\eta)$ into the complex plane.

Single-particle excitations associated with the injection or emission of an electron with wave vector k, $A^+(k,\omega)$ or $A^-(k,\omega)$, can be written in the spectral form

$$A^\pm(k,\omega) = \sum_n |\langle \psi_n^\pm | f_k^\pm | \psi_0 \rangle|^2 \delta[\omega \mp \omega^\pm], \qquad (4)$$

where $f_k^+ = f_k^\dagger$ and $f_k^- = f_k$. $|\psi_0\rangle$ is the ground state of a N-site system in the N_e-particle sector while $|\psi_n^\pm\rangle$ denote the nth excited states in the $N_e \pm 1$-particle sectors with excitation energies $\omega_n^\pm = E_n^\pm - E_0$.

Optical excitations, on the other hand, connect states in the same particle sector with a site-parity change. For a system with open boundary conditions (OBC) the regular part of the optical absorption

$$\sigma_{reg}(\omega) = \frac{\pi}{N} \sum_n \omega_n |\langle \psi_n | P | \psi_0 \rangle|^2 \delta[\omega - \omega_n] \qquad (5)$$

is related to the dynamical polarizability, $\sigma_{reg}(\omega) = \omega \alpha(\omega)$, where $P = -\sum_{j=1}^N j(f_j^\dagger f_j - 1)$ is the dipole operator (in units of e) and $\omega_n = (E_n - E_0)$. Then the current operator is obtained from $J = i[H, P]$. Applying periodic boundary conditions (PBC), the optical conductivity can be calculated from

$$\sigma_{reg}(\omega) = \frac{\pi}{N} \sum_n \frac{|\langle \psi_n | J | \psi_0 \rangle|^2}{\omega_n} \delta[\omega - \omega_n]. \qquad (6)$$

Note that for our fermion-boson model (1), the current operator has two contributions, $J = J_f + J_b$, where $J_f = it_f \Sigma_j f_{j+1}^\dagger f_j - f_j^\dagger f_{j+1}$ and $J_b = it_b \Sigma_j f_{j+1}^\dagger f_j b_j^\dagger - f_j^\dagger f_{j+1} b_j + f_{j-1}^\dagger f_j b_j^\dagger - f_j^\dagger f_{j-1} b_j$. The f-sum rule

$$S_{reg}(\infty) + \pi D = -\pi E_{kin}/2 \qquad (7)$$

connects the frequency-integrated optical response $S_{reg}(\omega) = \int_0^\omega \sigma_{reg}(\omega') d\omega'$ to the kinetic energy $E_{kin} = \frac{1}{N} \langle 0 | H - \omega_0 \Sigma_i b_i^\dagger b_i | 0 \rangle$, where the Drude part $\propto D$ serves as a measure for coherent transport. For OBC, only a D precursor exists in the metallic region.

In the actual DDMRG calculation of spectral functions the required CPU time increases rapidly with the number of the density-matrix eigenstates m. Since the DDMRG approach is based on a variational principle,[15] we first of all have to prepare a good "trial function" for the ground state with as many density-matrix eigenstates as possible. As a rule we keep $m \sim 500$ states to obtain the true ground state in the first five DDMRG sweeps and afterwards take $m \sim 200$ states for the calculation of the various spectra from Eq. (3) with a broadening $\eta = 0.1$. In order to save CPU time in the DDMRG runs we take into account just $n_b = 3$ pseudosites. In this case the n_bth local boson pseudosite density is smaller than 10^{-5}. Using $n_b = 4$ this value can be reduced to 10^{-8}

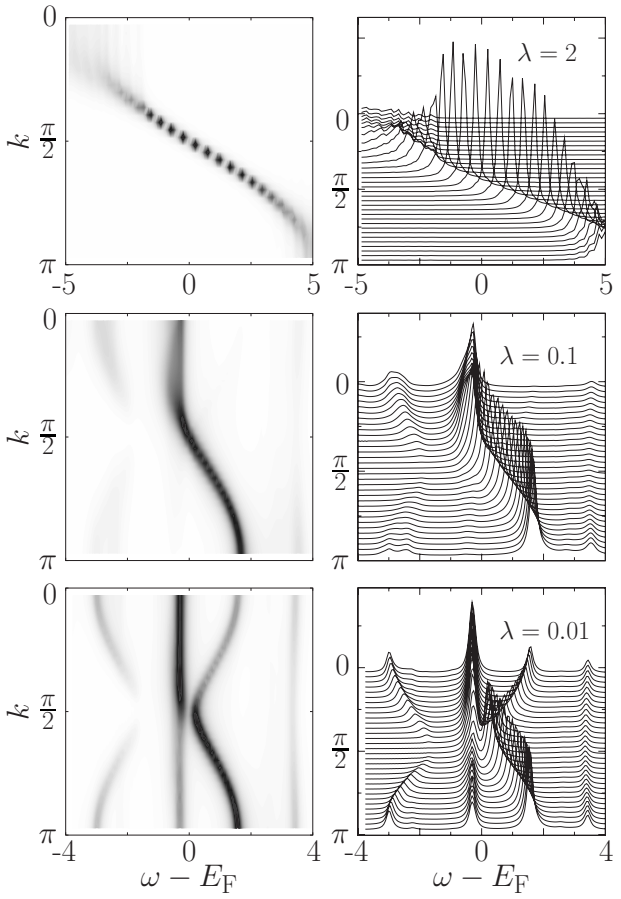

FIG. 2. Intensity (left panels) and line-shape (right panels) of the single-particle spectral function $A(k,\omega)$ in the half-filled band sector of the fermion-boson transport model (1) on a $N=32$-site chain. The upper two rows (lower row) give DDMRG data for $\lambda=2$ and 0.1 in the metallic regime ($\lambda=0.01$, insulating regime), where $\omega_0=2$. All energies are measured in units of t_b. Since we apply OBC, we use quasimomenta $k=\pi l/(N+1)$ with integers $1\leq l\leq N$.

which leads, however, not to visible change in the spectra because the discarded weight in the DDMRG calculations is $\sim 10^{-3}$ (i.e., three orders of magnitude larger than for the DMRG ground-state calculations).

III. RESULTS

A. Photoemission spectrum

Let us first discuss the single-particle spectra of the transport model (1) in the regime where the background is stiff, i.e., the distortions induced by the particle hopping process are energetically costly ($\omega_0=2$).

For very large λ the free transport channel nevertheless dominates and an almost particle-hole symmetric spectrum $[A^+(k,\omega-E_F)\sim A^-(k-\pi,E_F-\omega)]$ results (see Fig. 2 upper panels). As λ decreases, the background distortions hardly relax. Consequently, the bosonic degrees of freedom will strongly affect the transport. The middle panels of Fig. 2 show how, at $\lambda=0.1$, strong correlations develop in the occupied states probed by photoemission (PE) for $\omega<E_F$. The introduced hole can only move coherently by the six-step process [Eq. (2)], where in steps one-three, three bosons were excited, which are consumed in steps four-six afterward. In this way the collective particle-boson dynamics leads to a flattening of the "coherent" band for $k\leq k_F$. By contrast an additional electron, which probes the unoccupied states in an inverse (I)PE experiment ($\omega>E_F$), can more easily move by a two-step process, even if pronounced CDW correlations exist in the background medium.[12] The incoherent parts of $A(k,\omega)$ far away from the Fermi energy E_F are caused by excitations with additional bosons involved (bear in mind that the ground state with N_e electrons is a multiphonon state and the wave vector of the $N_e\pm 1$ target state corresponds to the total momentum of electrons and bosons).

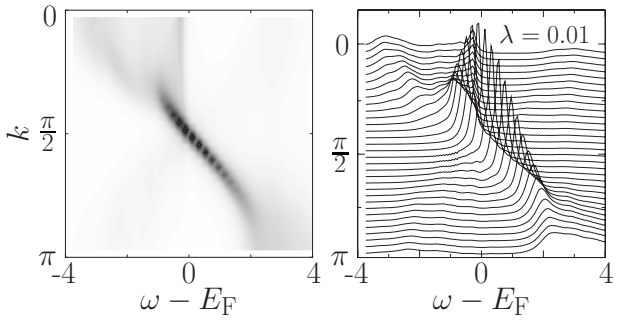

FIG. 3. Density (left) and line-shape (right) plot of the $A(k,\omega)$ spectra. Again $N=32$ (OBC), $\lambda=0.01$, but now $\omega_0=1$.

While for $\lambda=0.1$, $A(k_F,\omega)$ has finite spectral weight at E_F, i.e., the system is still metallic (albeit the TLL charge exponent K_ρ is noticeably reduced from one[13]), an excitation gap opens in the PE spectrum as λ falls below a certain critical value, provided that $\omega_0>\omega_{0,c}(\lambda=0)$.[13] We find $\lambda_c(\omega_0=2)\simeq 0.05$. The lower panels of Fig. 2 show $A(k,\omega)$ for $\lambda=0.01$, in the insulating regime, where a CDW with true long-range order exists. The TLL-CDW quantum phase transition is driven by the correlations that might evolve in the background medium at commensurate fillings. Let us emphasize the dynamical aspect of this process: the (collective) bosonic excitations are intimately connected to the motion of the particles, and themselves have to persist long enough in order to affect the many-particle state.

The ARPES spectrum for the insulating state clearly shows the doubling of the Brillouin zone. The remaining asymmetry with regard to the spectral weight of the absorption signals as $k\leftrightarrow(\pi-k)$ vanishes for $\lambda\to 0$. Most notably the widths of the highest PE and lowest IPE coherent bands differ by a factor of about $(t_b/\omega_0)^4$ since the CDW order is restored if the injected hole [electron] is transferred to a NNN site by a process of order $O(t_b^6/\omega_0^5)$ $[O(t_b^2/\omega_0)]$. Hence the CDW state exhibits a correlation-induced asymmetric band structure.[12]

The strong interrelation of charge dynamics and background fluctuations becomes obvious if we decrease ω_0 below $\omega_{0,c}$ keeping $\lambda=0.01$ fixed. Of course, in passing the accompanied insulator-metal transition the PE spectrum changes completely but the "nature" of the TLL at $\omega_0=1$ is different compared to that of the metallic state realized at larger ω_0 and λ as well (cf. Fig. 3 and upper panels of Fig. 2). The single-particle spectrum for $\omega_0=1$ shows sharp ab-

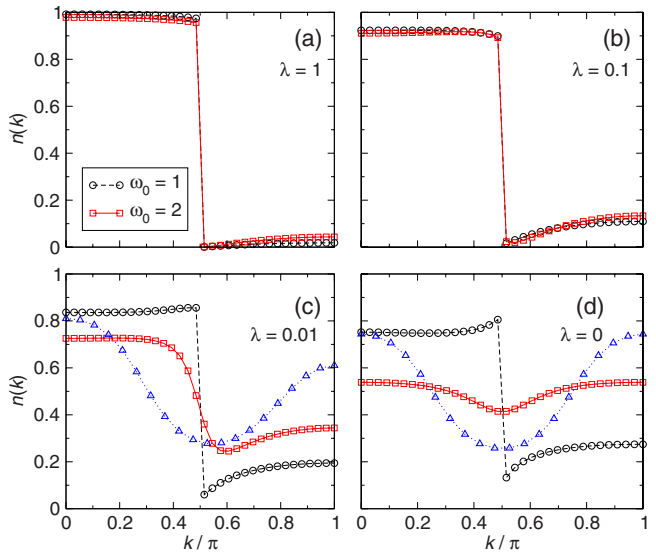

FIG. 4. (Color online) Momentum distribution function $n(k)$ for the half-filled two-channel transport model (1) with 66 sites and PBC, as λ decreases from one (a) to zero (d) at $\omega_0=1$ (circles) and 2 (squares). Triangles show $n(k)$ for a half-filled t-t'-U model (38 sites, PBC) with $U=10t'$, $t=t'$ [panel (c)], and $t=0$ [panel (d)] (see text). In order to obtain more accurate ground-state data we use $n_b=4$ pseudosites.

sorption signals in the vicinity of k_F only. In a wide k-space region emanating from $k=0$ ($k=\pi$) the PE (IPE) spectrum is smeared out (overdamped), i.e., here the dynamics of the system is dominated by bosonic fluctuations.

B. Momentum distribution function

The different transport behavior becomes also apparent in the momentum distribution function

$$n(k) = \frac{1}{N}\sum_{j,l} e^{ik(j-l)}\langle c_j^\dagger c_l\rangle. \quad (8)$$

By means of DMRG, the ground-state correlation function $\langle c_j^\dagger c_l\rangle$ can be easily calculated for PBC. Figure 4 displays $n(k)$ for two characteristic boson energies, above and below $\omega_{0,c}$.

In the former case, the TLL-CDW transition causes significant changes in the functional form of $n(k)$. For $\lambda>\lambda_c$, one expects an essential power law singularity at k_F, corresponding to a vanishing quasiparticle weight. For finite TLL systems the difference $\Delta=n(k_F-\delta)-n(k_F+\delta)$ is finite (with $\delta=\pi/66$ in our case).[16] Δ rapidly decreases approaching the CDW transition point with decreasing λ [see data for $\omega_0=2$ (red squares)]. In the CDW phase the singularity at k_F vanishes. Note that the periodicity of $n(k)$ doubles at $\lambda=0$, in accordance with a $R^{(6)}$ NNN-only hopping channel. To substantiate this reasoning we have included in Fig. 4 $n(k)$ data calculated for the 1D Hubbard model with additional NNN transfer t'. We see that $n(k)$ of the fermion-boson model (1) is in qualitative agreement with our data and previous results for the t-t' Hubbard model,[17] in particular, for the case $t=0$. The upturn in $n(k)$ for $k>k_F$ persists even in the metallic regime as long as NNN-hopping processes triggered by the (CDW) correlations in the background are of importance.

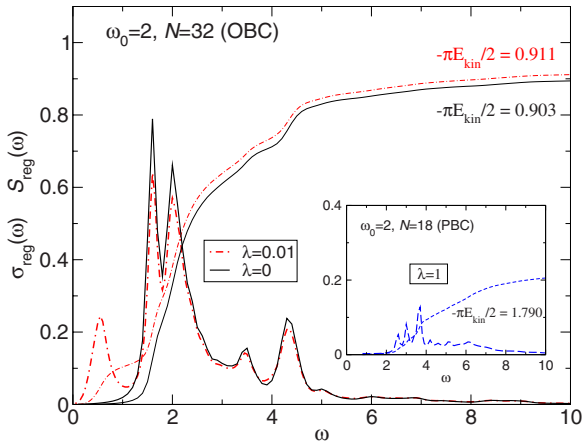

FIG. 5. (Color online) Optical conductivity $\sigma_{reg}(\omega)$ and integrated spectral weight $S_{reg}(\omega)$ in the half-filled transport model (1). The main panel (inset) displays DDMRG data for $\omega_0=2$ at $\lambda<\lambda_c$ ($\lambda\gg\lambda_c$), i.e., in the insulating (metallic) region, applying OBC (PBC).

For $\omega_0=1$ the system stays metallic for all λ. Besides the usual renormalization of $n(k)$ with increasing correlations (i.e., decreasing λ) we find a slight upturn in $n(k)$ for $k\lesssim k_f$. This might be attributed to the fact that in our model (1) a particle injected with $k=\pm\pi$ is almost unaffected by bosonic fluctuations (which holds also for the single-particle case[9]). So to speak the system behaves as a nearly perfect metal at this point. It is worth mentioning that an increase in $n(k)$ for both $k\lesssim k_F$ and $k\gtrsim k_F$ has also been found for the momentum distribution function of the Hubbard model (with and without magnetization) using the Gutzwiller variational wave function.[18]

C. Optical response

Finally we consider the evolution of the optical conductivity going from the correlated TLL to the CDW phase at $\omega_0=2$. The corresponding optical absorption spectra are depicted in Fig. 5. In the metallic state most of the spectral weight resides in the coherent Drude part. At $\lambda=1$ (see inset), we find $\pi D/N\simeq 1.6$, which has to be compared with $S_{reg}(\infty)\simeq 0.2$ (of course D decreases as λ gets smaller). In this case the wave-vector resolved single-particle spectra roughly extends from $\omega=-6$ to $\omega=6$. The regular part of the conductivity is mainly due to excitations to the phononic side bands appearing in the sectors with momenta far away from k_F. In the insulating region (see main panel), the first peak at about $\omega\simeq 0.5$ can be assigned to an optical excitation across the gap in the (coherent) two-band structure. These excitations are only accessible for $\lambda>0$. Additional excitations with higher energy occur around multiples of the boson frequency, where $\omega\simeq\omega_0=2$ sets an absorption threshold for the $\lambda=0$ case. As expected for an insulating system with OBC, the whole spectral weight is contained in $S_{reg}(\infty)\simeq-\pi E_{kin}/2$. We emphasize that the CDW state in our model contains less than one boson per site on average, unlike, e.g.,

the Peierls insulating state in the Holstein model. That is the CDW phase typifies rather as a correlated insulator—such as the Mott-Hubbard insulator—and no divergence occurs at the optical absorption threshold.[19]

IV. SUMMARY

In conclusion, we have determined the spectral properties of a highly nontrivial two-channel fermion-boson transport model for the 1D half-filled band case, using an unbiased DDMRG technique. The background medium, parameterized by bosonic degrees of freedom, strongly influences the charge-carrier dynamics, as it happens in many novel materials. If the background fluctuations dominate we find diffusive transport. In opposite case of strong background correlations coherent quantum transport may evolve on a reduced energy scale. These correlations can also trigger a metal-insulator transition. The insulating CDW state has an asymmetric band structure, leading to characteristic signatures in the ARPES and optical response. Whether an extended model with spinful fermions gives rise to an attractive metallic phase like in the Holstein-Hubbard model[20] would be an interesting question for further research.

ACKNOWLEDGMENTS

The authors would like to thank A. Alvermann, K. W. Becker, D. M. Edwards, F. Gebhard, G. Hager, E. Jeckelmann, S. Sykora, L. Tincani, S. A. Trugman, and G. Wellein for valuable discussions. This work was supported by DFG under Grant No. SFB 652 and the KONWIHR project HQS@HPC.

[1] M. Berciu, Phys. **2**, 55 (2009).
[2] C. L. Kane, P. A. Lee, and N. Read, Phys. Rev. B **39**, 6880 (1989).
[3] G. Martinez and P. Horsch, Phys. Rev. B **44**, 317 (1991).
[4] K. Wohlfeld, A. M. Oleś, and P. Horsch, Phys. Rev. B **79**, 224433 (2009).
[5] *Polarons in Advanced Materials*, Springer Series in Material Sciences Vol. 103, edited by A. S. Alexandrov (Springer, Dordrecht, 2007).
[6] N. Tsuda, K. Nasu, A. Fujimori, and K. Siratori, *Electronic Conduction in Oxides* (Springer-Verlag, Berlin, 2000).
[7] A. Weiße and H. Fehske, New J. Phys. **6**, 158 (2004).
[8] D. M. Edwards, Physica B (Amsterdam) **378-380**, 133 (2006).
[9] A. Alvermann, D. M. Edwards, and H. Fehske, Phys. Rev. Lett. **98**, 056602 (2007).
[10] S. A. Trugman, Phys. Rev. B **37**, 1597 (1988).
[11] J. Bonča, S. A. Trugman, and I. Batistić, Phys. Rev. B **60**, 1633 (1999).
[12] G. Wellein, H. Fehske, A. Alvermann, and D. M. Edwards, Phys. Rev. Lett. **101**, 136402 (2008); H. Fehske, A. Alvermann, and G. Wellein, in *High Performance Computing in Science and Engineering*, edited by S. Wagner, M. Steinmetz, A. Bode, and M. Brehm (Springer-Verlag, Berlin, 2009), pp. 649–668.
[13] S. Ejima, G. Hager, and H. Fehske, Phys. Rev. Lett. **102**, 106404 (2009).
[14] S. R. White, Phys. Rev. Lett. **69**, 2863 (1992).
[15] E. Jeckelmann, Phys. Rev. B **66**, 045114 (2002); E. Jeckelmann and H. Fehske, Riv. Nuovo Cimento **30**, 259 (2007).
[16] S. Ejima and H. Fehske, Europhys. Lett. **87**, 27001 (2009).
[17] C. Gros, K. Hamacher, and W. Wenzel, Europhys. Lett. **69**, 616 (2005).
[18] W. Metzner and D. Vollhardt, Phys. Rev. Lett. **59**, 121 (1987); M. Kollar and D. Vollhardt, Phys. Rev. B **65**, 155121 (2002).
[19] E. Jeckelmann, F. Gebhard, and F. H. L. Essler, Phys. Rev. Lett. **85**, 3910 (2000).
[20] M. Tezuka, R. Arita, and H. Aoki, Phys. Rev. Lett. **95**, 226401 (2005).